IMPROVEMENT AND VALIDATION OF A TRANSIENT MODEL TO PREDICT PHOTOVOLTAIC MODULE TEMPERATURE

Amanda Luketa-Hanlin
Sandia National Laboratories
P.O. Box 5800 MS 1033
Albuquerque, NM 87185
e-mail: ajluket@sandia.gov

Joshua S. Stein
Sandia National Laboratories
P.O. Box 5800 MS 1033
Albuquerque, NM 87185
e-mail: jsstein@sandia.gov

ABSTRACT

Module temperature is modeled using a transient heat-flow model. Module temperature predicted in this fashion is important in the calculation of cell temperature, a vital input in performance modeling. Parameters important to the model are tested for sensitivity, and optimized to a single day of measured module temperature using simultaneous non-linear least squares regression. These optimized parameters are then tested for accuracy using a year's worth of data for one location. The results obtained from this analysis are compared with modeled data from a different site, as well as to results obtained using a steady-state model. We find that the transient model best captures the variability in module temperature, and that the transient model works best when calibrated for a specific location.

1. INTRODUCTION

Cell temperature is the second most important factor, after irradiance, in determining the performance of a typical photovoltaic (PV) system. Models used to predict PV performance typically calculate cell temperature as a function of irradiance at the plane of array, ambient air temperature, wind speed, and a temperature offset representing the difference between back-of-module and cell temperatures. These formulations generally assume that cell temperature varies directly with these variables in a steady-state manner (e.g., changes in irradiance result in immediate and corresponding changes in cell temperature). While this approach was designed for and may be adequate when performance models use hourly averaged inputs, such as Typical Meteorological Year

(TMY) data, field measurements of module temperatures at higher sampling rates indicate that module and cell temperatures vary more slowly than irradiance and therefore a transient model of module (and cell) temperature may be more appropriate when performance is calculated at short time intervals.

This paper is organized as follows: In Section 2, we briefly describe the transient module temperature model first developed by Jones and Underwood [1] and which we consider in this evaluation. This model simulates module temperature as a balance between incoming heat and heat losses from electrical conversion, radiation, and convective heat transfer. The challenge in applying such a model lies in defining appropriate parameters to describe the module's thermal behavior.

In Section 3, we identify key input parameters that are generally unknown or difficult to estimate from the data provided on a manufacturer's data sheet. We run a set of parameter sensitivity analyses by independently varying selected parameters and illustrating how simulated module temperatures compare to field measurements made in Lanai, Hawaii.

In Section 4 we apply a multi-parameter, simultaneous, nonlinear optimization solver to estimate an optimal set of parameters that fit the model to temperature data measured on a single day in Lanai.

In Section 5, we test these optimal parameters by simulating approximately one year of module temperature data from Lanai and comparing these results with measured module temperatures. Additionally, we simulate one month of module temperature data from

Albuquerque, New Mexico using the optimal parameter values found in Lanai to test the importance of site-specific optimization.

In Section 6, we compare transient model results to those obtained using a steady-state model.

2. MODEL DESCRIPTION

Traditionally, steady-state models have been used to predict module temperature, using measured weather conditions. These models are simple to implement, yet are generally only applicable with hourly-averaged data since they cannot represent the transient heat flow processes at shorter time scales. Eq. (1) shows one such steady-state model developed at Sandia National Laboratories [2].

$$T_{module} = E \cdot \{e^{a+b \cdot WS}\} + T_{ambient} \quad (1)$$

This model uses ambient temperature $T_{ambient}$, irradiance E, and wind speed WS as inputs to calculate module temperature. The coefficients a and b (both less than zero) are empirically determined from observations, and are specific to the composition and construction of the module as well as to the mounting configuration (e.g., open rack vs. roof mount). Eq. (1) is the steady-state model that will be used in comparison with the transient temperature model [1] shown below in Eq. (2).

$$C_{module} \frac{dT_{module}}{dt} = q_{lw} + q_{sw} + q_{conv} - P_{out} \quad (2)$$

Here, C_{module} is the heat capacity of the module, q_{lw} is heat transfer due to long-wave radiation, q_{sw} is heat transfer due to short-wave radiation, q_{conv} is convective heat transfer, and P_{out} is electrical power generated by the module. dT_{module}/dt is the time derivative of module temperature. This time derivative is solved using the Euler method to calculate module temperature as a function of time:

$$T_{module}(t+1) = T_{module}(t) + step \cdot \frac{dT_{module}}{dt} \quad (3)$$

In Eq. (3), *step* represents the time step between each data point. This will usually be a constant value depending on the sampling rate, but is not required to be constant. The components of Eq. (2) are broken down as follows, with a list of nomenclature at the end of this paper.

$$C_{module} = \sum_m A \cdot \rho_m \cdot t_m \cdot C_m \quad (4)$$

$$q_{lw} = A \cdot \sigma \cdot \left[\left(\frac{1 + \cos\beta_{surface}}{2} \cdot \varepsilon_{sky} \cdot T_{sky}^4 \right) \right.$$
$$+ \left(\frac{1 - \cos\beta_{surface}}{2} \cdot \varepsilon_{ground} \right.$$
$$\left. \cdot T_{ground}^4 \right) - \left. (\varepsilon_{module} \cdot T_{module}^4) \right] \quad (5)$$

$$q_{sw} = \alpha \cdot \Phi \cdot A \quad (6)$$

$$q_{conv} = -(h_{c,forced} + h_{c,free}) \cdot A \cdot (T_{module} - T_{ambient}) \quad (7)$$

$$P_{out} = C_{FF} \cdot \frac{E_e \ln(k_1 E_e)}{T_{module}} \quad (8)$$

In Eq. (7) the forced convection, $h_{c,forced}$, represents the rate of heat loss from the module by convection. In the field this quantity is likely a function of wind speed across the module surface, and possibly thermal properties of the air. For this modeling analysis we assume that $h_{c,forced}$ can be represented as a simple linear function of wind speed:

$$h_{c,forced} = h_{forced} \times WS \quad (9)$$

3. SENSITIVITY ANALYSIS

Most of the parameters in the transient temperature model are either measured weather inputs, or can be found on the module manufacturer's data sheet. For our analysis we assumed parameter values given in [1], except as noted below. Some parameters, however, are either not readily measured nor accessible; these include the module's heat capacity, C_{module}, the temperature and emissivity of the sky, ε_{sky} and T_{sky}, the absorptivity of the module surface, α, and the forced convection coefficient, h_{forced}. The sensitivity of the transient model to each of these parameters is illustrated via a set of "one-off" analyses where one parameter is varied while keeping all other parameters fixed. Table 2 and Figures 1 – 7 show the results of these analyses. For each figure, the transient model is run for a typical day in Lanai, HI (in this case, March 25th, 2010) for a wide range of values of the targeted parameter. The predicted module temperature corresponding to high and low extremes for each parameter is plotted along with the measured module temperature for that day, in addition to predicted module temperature corresponding to the 'best-fit' value of the parameter being tested, where applicable. The best-fit

value is determined independently for each parameter by minimizing the root mean square error (RMSE) between predicted and measured module temperature. In Section 4, a simultaneous multi-parameter optimization analysis to rigorously determine the most accurate value for each parameter is described and the results are presented.

The following table shows the default (initial) values used for each parameter in the analysis; for example, when testing the sensitivity of the model to the absorptivity, α, the values used as inputs in the model for C_{module}, h_{forced}, ε_{sky} and T_{sky} (sky conditions) were taken from the table below. The module modeled in this analysis is constructed of crystalline silicon (cSi), polymer laminate, and glass.

TABLE 1: DEFAULT PARAMETER VALUES

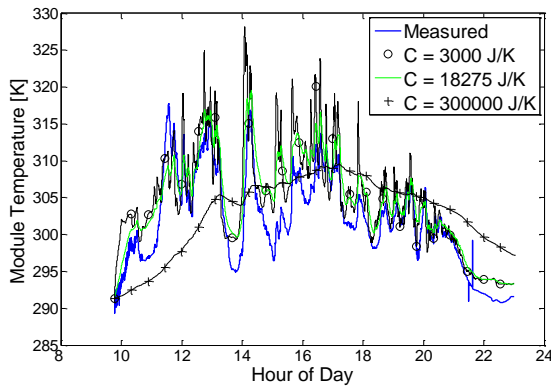| Parameter	Value
α	0.75
C_{module}	16,500 J/K
h_{forced}	6.67
Sky conditions	'cloudy'

Fig. 1: Sensitivity of model to changes in module heat capacity.

Figure 1 shows an example of how heat capacity affects the modeled temperature variability. A module with low heat capacity will experience more temperature variations with irradiance changes than a module with a high heat capacity.
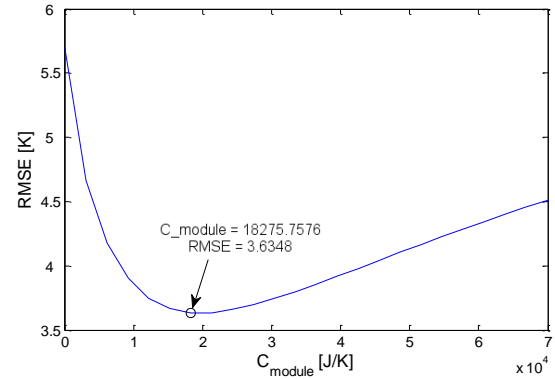

Fig. 2: Sensitivity of model to module heat capacity.

Figure 2 shows that unrealistically large or small values for the module's heat capacity result in a comparatively poor fit to measured temperatures. There appears to be a reasonable range of values (between 15000 and 30000 J/K) that produces an acceptable match to measured temperatures as measured with the RMSE statistic.
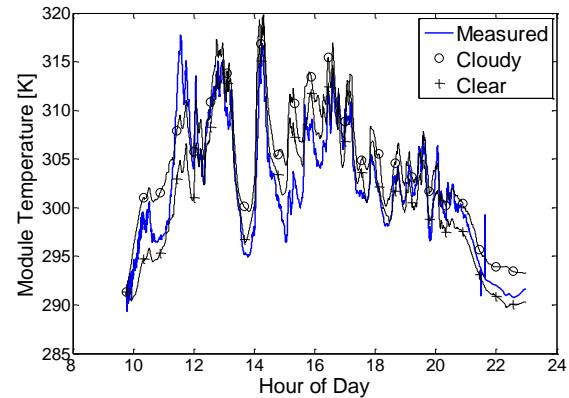

Fig. 3: Sensitivity of model to type of sky conditions, i.e. 'clear' or 'cloudy.'

Figure 3 shows how differences in the emissivity and temperature of the sky between clear and cloudy conditions affect the model results. Notice very little change in predicted module temperature between these two sky conditions; however, Table 2 shows that the RMSE values indicate that "cloudy" conditions results in a slightly better fit.

TABLE 2: SENSITIVITY RESULTS FOR SKY EMISSIVITY

Sky Condition	ε_{sky}	T_{sky}	RMSE
Clear	0.95	$T_{ambient} - 20K$	3.65
Cloudy	1.0	$T_{ambient}$	2.95

While the appropriate sky condition should be applied to the model if possible, this may prove difficult if using real-time data. From Table 2, the improvement in model accuracy by varying 'clear' or 'cloudy' sky conditions is not significantly large when compared with the effects of other parameters (absorptivity, Fig. 5, and forced convection coefficient, Fig. 7) that selection of clear or cloudy conditions is likely to be of primary concern. Incorrectly choosing 'clear' as the sky condition for the example day shown would only increase the RMSE by less than 1 degree K.

Fig. 4: Sensitivity of model to changes in absorptivity of module surface.

Figure 4 shows an example of how changes in module absorptivity affect simulated module temperature. The best-fit value for α is in between the high and low extremes possible – a low absorptivity results in almost no temperature variation, while a high absorptivity results in too much variation.
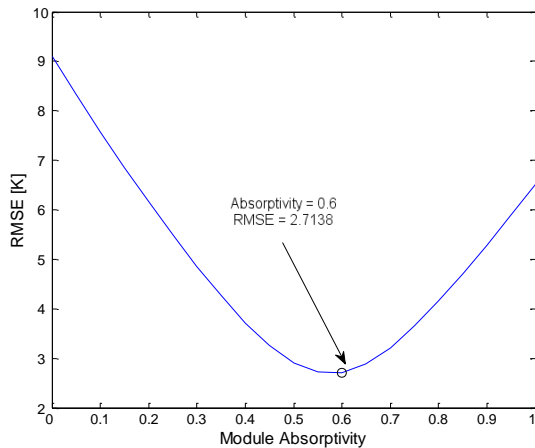

Fig. 5: Sensitivity of model to absorptivity of module surface.

From the results shown in Figure 5, it appears that α

around 0.6 is the most accurate; this value will vary depending on the material of the module.
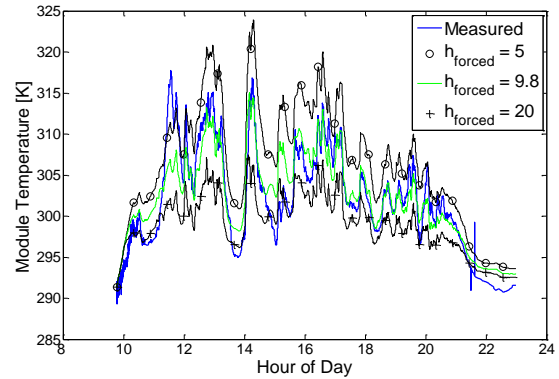

Fig. 6: Sensitivity of model to changes in the forced convection coefficient.

Figure 6 shows an example of how changes in the forced convection coefficient affect simulated module temperature. Lower values for h_{forced} result in generally higher module temperature due to less convective cooling; similarly, higher values for h_{forced} result in lower module temperature.
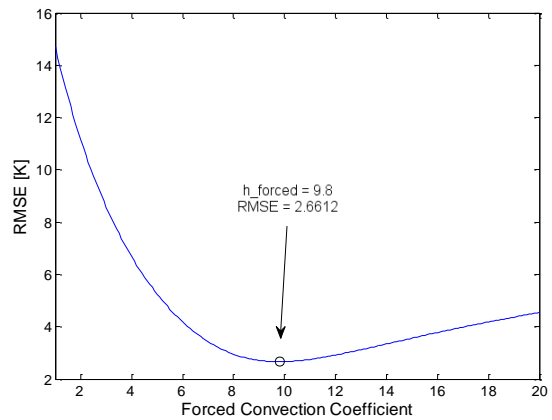

Fig. 7: Sensitivity of model to the forced convection coefficient.

From the results shown in Figure 7, the best-fit value for h_{forced} is 9.8. There appears to be a reasonably large coefficient range (between roughly 7.5 and 14) that produces RMSEs of about the same value.

4. MODEL CALIBRATION

In this section we describe an effort to estimate the values

4

of α, C_{module}, and h_{forced} simultaneously by applying a nonlinear least-squares optimization routine to the data measured on March 25th, 2010 in Lanai, HI.

The best-fit values obtained from the sensitivity study in Section 3, shown below in Table 3 along with the constraints placed on each parameter for the optimization, were used as initial parameter guesses. While these parameter values are the most accurate when taken independently of other inputs to the model, this is not necessarily the case when multiple inputs are varied simultaneously. Using these values should, however, provide a reasonable initial guess.

TABLE 3: SENSITIVITY STUDY RESULTS AND PARAMETER CONSTRAINTS

Parameter	Initial Value	Upper-Lower Bounds
C_{module}	18276 J/K	3,000 – 300,000
α	0.6	0 – 0.8
Sky conditions	'cloudy'	N/A
h_{forced}	9.8*WS	1–50

We then applied the nonlinear least-squares solution algorithm, *lsqnonlin*, from Matlab's Optimization Toolbox. This optimization algorithm converged and the results are shown below in Table 4.

TABLE 4: OPTIMIZATION CONSTRAINTS AND RESULTS

Parameter	'Optimal' value
C_{module}	22,280 J/K
α	0.8
h_{forced}	$10.65 \times WS$

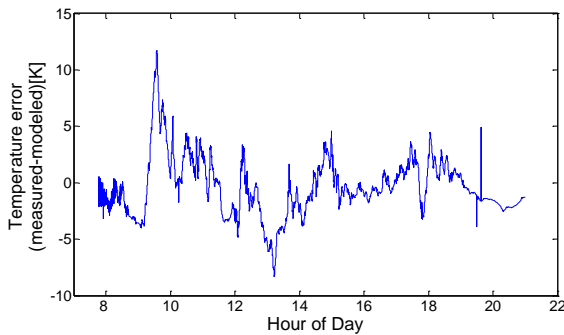Figure 8 compares the model error (measured-modeled) over time for the optimized set of parameters.

Fig. 8: Optimized model error over time for March 25th, 2010, Lanai, HI.

For the majority of the representative day, the modeled module temperature obtained using the results from the optimization study is reasonably accurate, generally

staying within 5 degrees K of the measured module temperature.

5. VALIDATION

The transient model was tested using the optimized results from Table 4 with data from Lanai, HI for each day in 2010. Weather data (i.e., irradiance, air temperature, and wind speed) were measured at 1-minute intervals; back-of-module temperature was also measured at 1-minute intervals. Figure 9 shows the RMSE between measured and modeled module temperature for each day of the year for which data is available (292 days).
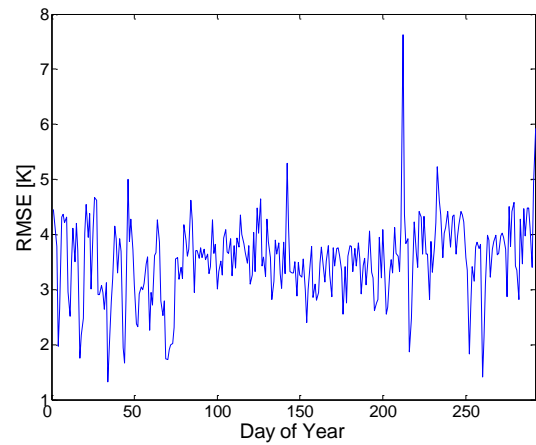

Fig. 9: RMSE of module temperature for days in 2010, using data from Lanai, HI. Generally, the RMSE is approximately 4 degrees K or less with few exceptions.

Figure 10 below repeats the same procedure using the optimized results for Lanai, except applied to one month of data collected in Albuquerque, NM. The results show, clearly, that parameter values optimized for one location are not necessarily applicable to other locations. However, from Figure 9 it appears that this calibration must be done only once using a representative day in order to produce consistent and reasonable results on a yearly basis.
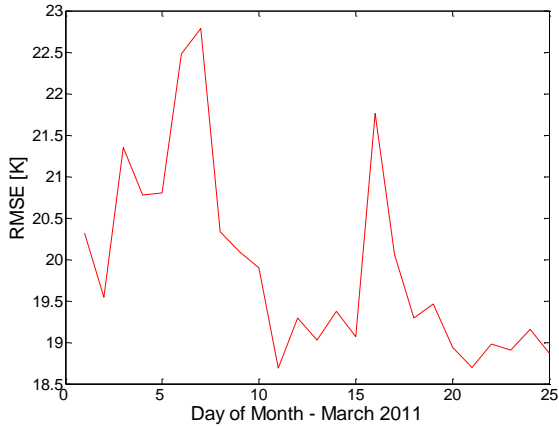
Fig. 10: RMSE for most of March 2011 using optimized Lanai results applied to Albuquerque. The model is neither accurate nor consistent in its level of accuracy.

6. STEADY STATE MODEL COMPARISON

Figure 11 compares measured module temperatures with simulated results from both a selected steady-state model and the improved transient model developed here. The comparison in Figure 11 uses the same data collected in Lanai for March 25, 2010 at a 1-second time interval. The transient model uses input parameters resulting from the previous optimization study; the predicted module temperature calculated using the steady-state model is based off of Eq. (1) with a = -3.56 and b = -0.075. Both models use the same weather data (irradiance, wind speed, and ambient temperature) as inputs. It is clear that the steady-state model greatly overestimates the variability in module temperature. If such a steady-state model was applied to the prediction of PV power output (e.g., for a grid integration study), it would overestimate the variability in power to some degree, due to exaggeration of the predicted module and cell temperature fluctuations. Using the improved transient module temperature model developed here provides a better representation of module temperature variability, which may be significant when making predictions with a short time step.
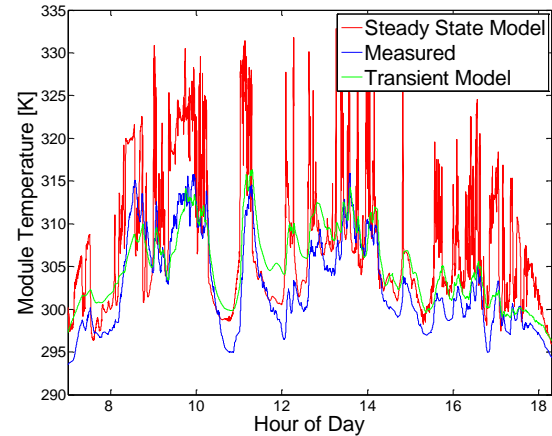

Fig. 11: Comparison of steady-state and transient module temperature models.

Figure 12 shows the temperature errors for each model. Although both models tend to over-predict temperature during clear-sky periods, it is clear that the transient model more accurately predicts module temperature. The negative bias in Figure 12, especially evident in the steady-state model results, will result in generally higher module temperatures and consequently lower predicted module efficiency.
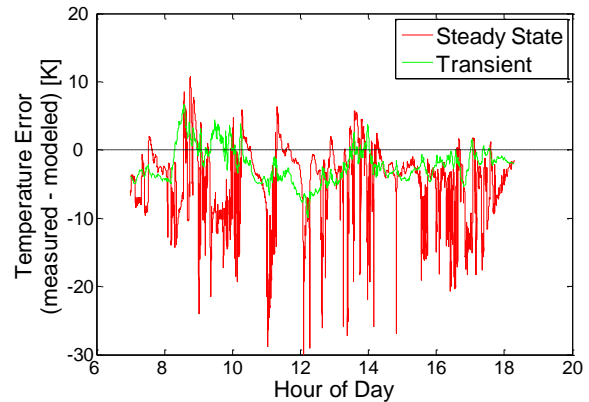

Fig. 12: Errors between measured and predicted module temperature for each model.

7. SUMMARY AND CONCLUSIONS

We have shown that a transient model for module temperature [1] can reasonably predict module temperature when calibrated using site-specific data. We compared the calibrated transient temperature model to a steady-state temperature model and found that the steady-state temperature model exaggerates the variability in

predicted module temperature. This variability in predicted module temperature can translate into calculated cell temperatures that are artificially high; depending on the degree of temperature over-prediction, expected performance for a system can be either marginally or significantly lower than actual performance. The transient temperature model offers a greatly improved representation of the variability in module temperature which may significantly improve the quality of PV power simulations at short time scales.

8. FUTURE WORK

We have not determined how much site-specific data is required to calibrate the transient model. Convective cooling will be influenced by environmental conditions other than wind speed that affect the heat transfer properties of air, e.g., relative humidity. Because the transient model's accuracy is sensitive to forced convection, it may be necessary to obtain measured temperatures and concurrent weather for various weather conditions (e.g., humid and dry) to properly calibrate the model. Additionally, we assumed a simple linear relationship between the forced convection and wind speed; for improved model accuracy, this relationship may in fact be more complicated.

Our parameter estimation process minimized RMSE but in one instance (Figure 12) a residual bias in model predictions is evident. Future efforts may examine the parameter estimation process in order to address model biases.

9. NOMENCLATURE

α	absorptivity of module surface
$\beta_{surface}$	tilt angle of module from horizontal
ε_{ground}	emissivity of the ground surface
ε_{module}	emissivity of the module
ε_{sky}	emissivity of the sky dome
σ	Stefan-Boltzmann constant (5.669×10^{-8} W/m^2 K^4)
Φ	total incident irradiance on module surface (W/m^2)
ρ_m	density of material (kg/m^3)
a	steady-state model coefficient that determines the upper boundary for module temperature at high irradiance and low wind speeds
b	steady-state model coefficient that determines the rate at which module temperature drops as wind speed increases

A	module area (m^2)
C_{FF}	fill factor model constant (1.22 K m^2)
C_m	specific heat capacity of material (J/kg K)
E	Solar irradiance incident on module surface (W/m^2)
E_e	incident irradiance (W/m^2)
$h_{c,forced}$	forced convection (W/m^2 K)
h_{forced}	forced convection coefficient (J/m^3 K)
$h_{c,free}$	free convection (W/m^2 K) Equal to 1.31 [W/m^2 K$^{3/2}$] $\cdot$(T_{module} [K] $-$ $T_{ambient}$ [K])$^{1/3}$
k_1	constant, 10^6 m^2/W
t_m	thickness of material (m)
$T_{ambient}$	ambient temperature (K)
T_{ground}	ground temperature (K)
T_{module}	module temperature (K)
T_{sky}	effective sky temperature (K)
WS	wind speed at height of 10 meters (m/s)

10. ACKNOWLEDGMENTS

11. REFERENCES

1. A.D. Jones and C.P. Underwood, "A Thermal Model for Photovoltaic Systems." *Solar Energy* Vol. 70 No. 4, 2001.
2. D.L. King, W.E. Boyson, and J.A. Kratochvil, "Photovoltaic Array Performance Model." Sandia National Laboratories Report, SAND2004-3535, 2004.